Soft Matter

Polymer stabilization of cholesteric liquid crystals in the oblique helicoidal state

Journal:	*Soft Matter*
Manuscript ID	SM-ART-06-2018-001278.R1
Article Type:	Paper
Date Submitted by the Author:	10-Aug-2018
Complete List of Authors:	Rumi, Mariacristina; AFRL, RXAP Bunning, Timothy; Air Force Research Laboratory, White, Tim; University of Colorado, Chemical and Biological Engineering

Journal Name

ARTICLE

Polymer stabilization of cholesteric liquid crystals in the oblique helicoidal state

Received 00th January 20xx,
Accepted 00th January 20xx

DOI: 10.1039/x0xx00000x

www.rsc.org/

Mariacristina Rumi,[a,b] Timothy J. Bunning [a] and Timothy J. White *[c†]

Electrical control of the pitch has been reported in a variant of the cholesteric liquid crystal phase composed of chiral dopants and liquid crystal dimers with a bent conformation, such as CB7CB. For a finite range of applied electric field, the dimeric mesogens assume an oblique helicoidal structure, in which the helical axis is aligned along the electric field and the local director is tilted towards the helical axis (rather than being perpendicular to it). An electric field can directly regulate the periodicity (pitch), allowing reconfiguration of the optical response from a scattering or transparent state to a reflective state. Here, we employ polymer stabilization to retain the oblique helicoidal state absent an applied field. The polymer stabilized oblique helicoidal structures were investigated under various conditions and material compositions. With polymer stabilization, the magnitude of the selective reflection is found to be dependent on the strength of the applied field. Comparison of the electro-optical response of samples with and without a polymer network elucidates the relative role of boundary conditions, anchoring strength, and elastic energy on the stability of the oblique helicoidal state.

1. Introduction

Liquid crystal (LC) dimers are molecules in which two rigid rod-like units (e.g., oligophenylenes) are linked by a flexible spacer (e.g., an alkyl chain). Molecules in this class can be mesogenic and they often exhibit even-odd effects related to the spacer length, for example in phase transition temperatures.[1, 2] LC dimers have long been studied and their properties are often contrasted to those of their "monomeric" analogues. Recently, interest in LC dimers was invigorated by the discovery of a new type of liquid crystal phase, called the twist-bend nematic phase, which can exist below the traditional nematic phase for some LC dimers. Most of these studies have been based on the molecule 4',4"-(heptane-1,7-diyl)-dibiphenyl-4-carbonitrile, commonly referred to as CB7CB[3-7] (where CB stand for "cyanobiphenyl" and 7 is the number of CH_2 groups in the linker) and shown in Fig. 1a. Notably, CB7CB has a bent molecular conformation, which in part allows this molecule to exhibit the twist-bend nematic phase.[5, 6] Other LC dimers of this class, CB*n*CB, also assume a bent conformation if the number of methylene groups in the spacer, *n*, is odd. However, if *n* is even, the dimers are approximately linear. Thus, LC dimers with odd *n* have different molecular anisotropy than dimers with even *n* and monomeric analogues.

LC dimers with odd *n* exhibit elastic constants with different magnitudes and temperature dependences relative to those in rod-like LCs. Specifically, the bend elastic constant K_{33} is much smaller than in typical calamitic LCs and is also smaller than the twist elastic constant K_{22} ($K_{33} << K_{22}$).[4, 5, 8] For the canonical liquid crystal 5CB, K_{33} = 8.2 pN[9] and K_{33}/K_{22} = 2.2 at 25 °C.[10] In contrast, for CB7CB, $K_{33} \approx$ 0.3-0.4 pN[11, 12] and $K_{33}/K_{22} \approx$ 0.12 at 106 °C[11] and 0.17 at 103 °C.[12] In addition, K_{33} decreases drastically when the temperature is decreased from the clearing point, reaches a minimum about 1.5 °C above the transition to the twist-bend phase, and then it increases by a smaller amount as the transition is approached.[12] K_{33}/K_{22} remains below 1 throughout the nematic range.

In cholesteric (chiral nematic) liquid crystals (N*), the liquid crystal director rotates around a preferential direction (helical axis) in a sense determined by the chirality of the chiral dopant or the chiral liquid crystal molecules. The director completes a full rotation over a period p_0, the pitch, and is perpendicular to the helical axis (Fig. 2a). The director arrangement of this conventional form of the phase has been called a "right-angle helicoid".[4] It was predicted by Meyer in 1968[13] that, in a chiral nematic liquid crystal with $K_{33}/K_{22} < 1$, the right-angle helicoid is no longer the energetically favored structure for certain values of the electric field. Instead, for field strengths between a lower and an upper critical value, an "oblique helicoid" structure becomes the stable configuration, with the director forming a tilt angle $\theta < 90º$ with the helical axis (Fig. 2b). The helical axis is parallel to the electric field. Under these conditions, the tilt angle is field dependent as is the pitch ($p_E \neq p_0$).

[a] Air Force Research Laboratory, Materials and Manufacturing Directorate, Wright-Patterson AFB, Ohio 45433, United States.
[b] Azimuth Corporation, 4027 Colonel Glenn Highway, Beavercreek, Ohio 45431, United States.
† Email: Timothy.White.24@us.af.mil.

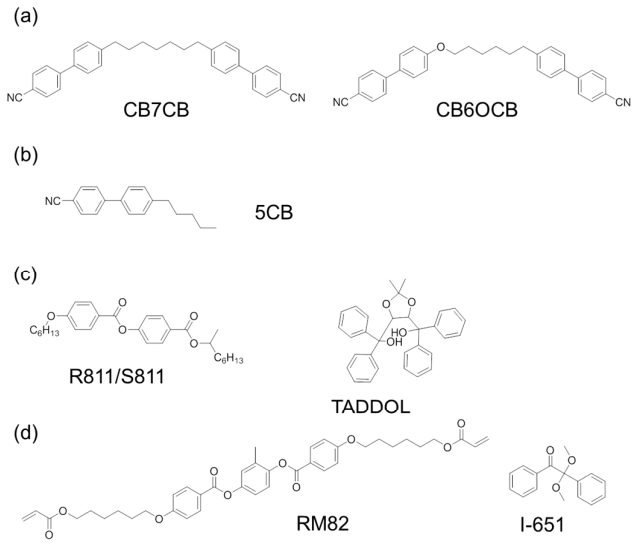

Fig. 1 Molecular structure of the materials used in the investigation: (a) LC dimers CB7CB and CB6OCB; (b) calamitic LC component 5CB; (c) chiral dopants (R811, S811, or TADDOL); and (d) reactive mesogen RM82 and photoinitiator Irgacure 651 (DMPA).

Only recently has the existence of this variant of the cholesteric phase been realized experimentally.[11, 14] It was shown that a mixture of CB7CB and the chiral dopant S811 exhibits this field-induced oblique helicoidal structure, with a pitch dependence consistent with Meyer's predictions ($p_E \propto 1/E$, where E is the amplitude of the electric field).[11, 14] If the helical axis is perpendicular to the cell substrates, the oblique helicoidal structure displays a selective reflection whose color is tunable by varying the electric field. Electrically induced tuning of the selective reflection from an oblique helicoid has also been observed in mixtures of CB7CB, CB6OCB (see Fig. 1a for the structure), 5CB, and S811, for which tuning ranges spanning several hundreds of nanometers in the visible and near infrared regions have been reported.[15] The oblique helicoidal state can also be established with a magnetic field and tuning achieved by varying the field strength.[16] Here, we will employ the nomenclature of Lavrentovich and colleagues by abbreviating this state as Ch_{OH} ("CH" for cholesteric and "OH" for oblique helicoid).[8, 12]

The pitch change of the oblique helicoidal structure is distinct from the pitch dilation exhibited by right-angle helicoidal N* systems when the field direction is perpendicular to the helical axis. At zero field and for fields below the lower critical value, the right-angle structure with helical axis parallel to the field direction is energetically favored even for systems with $K_{33}/K_{22} < 1$. For a sample with planar alignment and field directed through the thickness, this leads to the formation of the scattering focal conic texture at relatively low field strength. In this texture, the helical axis lies in the plane of the substrate but with an orientation that is random within that plane and different in each domain, as is the case for the familiar N* systems with $K_{33}/K_{22} > 1$. Above the upper critical field, all the molecules are oriented homeotropically along the field and the sample is transparent. The Ch_{OH} state exists in the intermediate field regime. The field-dependence of the Ch_{OH} pitch can be exploited in various types of dynamically tunable optical devices.[15, 17]

In this work we demonstrate that a device with an LC in an oblique helicoidal state that is stable in the absence of fields can be obtained by means of polymer stabilization. This is achieved by creating a crosslinked polymer network in situ while the LC system is in the field-induced Ch_{OH} state. After the polymerization is complete and the electric field is switched off, the LC system retains the same conformation it had during the network formation. The conditions to successfully achieve stabilization of the oblique helicoidal state and the optical and electro-optical properties of the resulting structures will be discussed.

Polymer stabilized liquid crystals (PSLCs) are composite materials in which an aligned polymer network is present within the low-molecular weight liquid crystalline phase. This is usually achieved by mixing polymerizable mesogens with non-reactive LCs, allowing the system to assume the desired ordered state, and then activating the polymerization of the reactive species.[18, 19] It is known that, if the polymerization conditions are chosen judiciously, the polymer network that forms has the same long-range orientation that the low-molecular weight precursors assumed at the onset of the polymerization,[20, 21] possibly with only a small decrease in the local order parameter relative to the pre-polymerization state.[22] Relatively small amounts of mesogenic polymer precursors, typically less than 10 wt%, are sufficient to effectively freeze the LC order in the formed polymer networks. The network consists of interconnected polymer fibrils that are distributed through the sample. The low-molecular weight components of the mixture surround and swell the fibrils.[19, 21] The properties of the PSLC composites are usually different from those of the systems before polymerization. For example, phase transitions are often

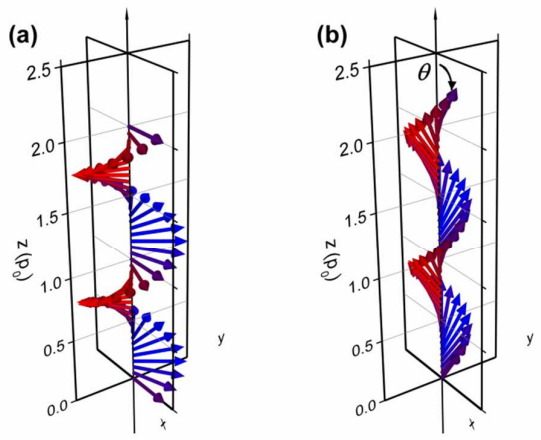

Fig. 2 Schematic display of the director orientation of a chiral nematic liquid crystal over two pitch lengths p_0: (a) right-angle helicoid, N*; (b) oblique helicoid, Ch_{OH}, with $\theta = 35°$. The director is shown as an arrow for ease of viewing (configurations with arrows flipped are actually equivalent). The reddish or bluish color represents arrows with opposite signs of the y component; purple, arrows with $y = 0$.

suppressed in PSLCs, which usually retain some degree of local order even when heated well above the clearing temperature of the starting material.[22-24] This can be explained by the alignment of the polymer chains in the network itself and the anchoring the network provides to the surrounding low-molecular weight liquid crystal molecules.[21, 25] The non-polymerized components can be removed from polymer stabilized samples and the polymer scaffold refilled with a different material. The anchoring to the polymer network can be strong enough to impose its order, at least in its vicinity, on the LC molecules used in the refilling step, even if these would have assumed a different alignment or texture in the absence of the network.[26, 27]

2. Experimental section

The molecular structures for the materials used in this study are shown in Fig. 1. CB7CB and CB6OCB (both from Synthon Chemicals) are LC dimers that have been previously employed to realize the Ch_{OH} state.[11, 15] They differ in the type of linker between the biphenyl units (Fig. 1a). The dimers were mixed with 5CB (TCI America), a well-known calamitic nematic liquid crystal (Fig. 1b). Mixing the dimers with 5CB decreases the phase transition temperature to near room temperature.[15] Various chiral dopants were added to this mixture, including R811, S811, and TADDOL (Fig. 1c). The polymer stabilizing network was prepared by photopolymerization of the reactive mesogen RM82 (1,4-bis-[4-(6-acryloyloxyhexyloxy)benzoyloxy]-2-methylbenzene; Synthon, ST00975), initiated with Irgacure 651 (2,2-dimethoxy-1,2-diphenylethan-1-one, Ciba) (Fig. 1d). Commercial alignment cells with 20 μm thickness and planar alignment (type SG100A200uG180 or S100A200uG180, Instec) were filled with the mixtures in the isotropic state and under red light, in order to avoid unintentional polymerization of the diacrylate.

Polymerization was induced by exposure to light from an LED with central wavelength at 365 nm and a bandwidth of 10 nm (Omnicure LX400+, Lumen Dynamics), incident on the sample at about 20° from the normal. The oblique angle allowed for the monitoring of the spectroscopic properties of the samples at normal incidence during photopolymerization, using an approximately collimated and unpolarized white light beam delivered through optical fibers and lenses to the sample and then detected by a modular spectrometer unit (USB2000+ or USB4000, Ocean Optics; range: 350-1000 nm). Transmission spectra were not corrected for reflection losses and the baseline was obtained with no cell in the light path. For measurements in the transmission mode with circularly polarized light, the polarization of the incident beam was controlled by a combination of a Glan-Laser calcite polarizer and a Fresnel rhomb. For measurements in the reflection mode, the incident light was unpolarized and the reflected light was sent through a Fresnel rhomb and a polarizer to separate the right-handed and left-handed circularly polarized components, which were independently detected.

The temperature of the samples during both polymerization and spectroscopic characterization was controlled by a heating stage (HCS402, Instec). A function generator (Agilent 33120A) and amplifier (MTS M93100 or M94100; Mound Technical Solutions) were used to apply a voltage to the alignment cells. Unless otherwise noted, the voltage was a square wave at 1 kHz frequency (no DC offset, 50% duty cycle); the field magnitude is reported as amplitude of the wave. Micrographs were obtained with polarizing optical microscopes (Nikon Optiphot-Pol or Eclipse 50iPol) in transmission or reflection mode.

Due to the diversity of the mixtures investigated, we employ a labeling scheme: OB# (where # is an integer) refers to a mixture of a given composition in a cell before exposure to UV light; PS-OB# refers to the same mixture and cell after it was exposed to UV light to form the polymer network. The nomenclature, composition, and photopolymerization conditions are summarized in Table 1.

Table 1 Composition of samples OB# and photopolymerization conditions used to produce PS-OB#.

Sample ID	Composition [a]						Exposure conditions [c]
	CB7CB	CB6OCB	5CB	Chiral dopant [b]	RM82	I-651	
OB1	25.1%	21.9%	46.1%	2.0% (R811)	4.0%	1.0%	E = 0.88 V/μm; I = 3.5 mW/cm^2 for 180 s
OB2, OB3	24.9%	21.8%	45.3%	3.6% (S811)	3.2%	1.2%	E = 1.60 V/μm; I = 3.5 mW/cm^2 for 180 s
OB4	24.9%	21.8%	45.3%	3.6% (S811)	3.2%	1.2%	E = 1.32 V/μm; I = 3.5 mW/cm^2 for 180 s
OB5	24.0%	22.8%	46.6%	3.4% (R811)	2.2%	1.0%	E = 1.32 V/μm; I = 4.3 mW/cm^2 for 180 s
OB6	24.9%	21.8%	45.3%	3.6% (S811)	3.2%	1.2%	E = 1.60 V/μm; I = 2.4 mW/cm^2 for 60 s
OB7	23.5%	22.5%	48.8%	1.0 (TADDOL)	3.4%	0.7%	E = 1.46 V/μm; I = 4.3 mW/cm^2 for 180 s
OB8	23.6%	23.0%	47.5%	1.1% (TADDOL)	3.8%	1.0%	E = 1.11 V/μm; I = 5.2 mW/cm^2 for 180 s
OB9	25.3%	21.8%	46.1%	2.1% (S811)	3.9%	0.9%	E = 0.72 V/μm; I = 3.5 mW/cm^2 for 180 s
OB10	24.6%	20.9%	46.2%	3.6% (R811)	4.0%	0.8%	E = 1.64 V/μm; I = 3.5 mW/cm^2 for 180 s
OB11	25.0%	21.0%	45.6%	3.5% (S811)	3.9%	0.9%	E = 1.51 V/μm; I = 3.5 mW/cm^2 for 180 s

(a) The content is expressed in wt% to one decimal place (the sum may differ from 100% due to rounding).
(b) The type of chiral dopant used is given in parenthesis after the amount.
(c) Each entry lists the electric field magnitude (E), intensity of UV light (I), and duration of the exposure used for the photopolymerization.

S811 is the chiral dopant used in prior investigations of the Ch_{OH} state.[11, 15] We also used R811, in order to test the polarization dependence of the reflection band, and TADDOL, to test that the existence of the state is not linked to a specific chiral dopant. TADDOL has larger helical twisting power than S811/R811, so smaller amounts are needed to obtain the same pitch. For the R811/S811 samples, the pitch can be estimated to be between 3.8 μm (2.0% case) and 2.1 μm (3.6% case), assuming an helical twisting power of 13 μm^{-1}.[14]

3. Results and discussion

3.1 Polymer stabilization in oblique-helicoid cholesterics

The goal of this work is to elucidate the contribution of polymer stabilization to the electro-optical response of the oblique helicoidal state of cholesteric liquid crystals. The properties of mixtures of CB7CB, CB6OCB, 5CB, a chiral dopant, RM82, and I-651 were examined before the formation of the polymer network. These mixtures are in the cholesteric liquid crystal phase (right angle helicoid) from 20-22 °C to 66-68 °C, above which they are isotropic. This phase behavior is similar to that reported for mixtures that did not include the reactive mesogen.[15] Transmission spectra as a function of electric field for sample OB1 at 23 °C are shown in Fig. 3a. During the measurement, a long-pass filter with cutoff at 400 nm was inserted to block the UV portion of the spectrometer's light source, in order to avoid unintentional photopolymerization of RM82. For $E \geq 1.60$ V/μm, sample OB1 was transparent and the transmission spectrum was featureless. At $E = 1.41$ V/μm, a small dip in transmittance was visible at 532 nm. The position of this band shifted to longer wavelengths with decreasing field amplitude. For $E = 0.66$ V/μm the band moved outside the detector range and for $E < 0.5$ V/μm (not shown in the figure), the sample became scattering.

It should be mentioned that p_E is expected to be significantly smaller than p_0, as a result of a large discontinuous change in pitch at the transition between the N* and Ch_{OH} states.[14] Thus, for a sample to exhibit a Ch_{OH} transmission notch in the visible range, the corresponding N* notch (at $E = 0$) needs to be in the mid IR range, which explains the choice of chiral dopant content used in this investigation (Table 1). When present, the position of the transmission notch is inversely proportional to the field amplitude (Fig. 3b), as expected.[15] The appearance of this transmission band in OB1 and its electric field dependence are taken as proof of the existence of the Ch_{OH} structure. This was typically observed up to 35-40 °C; at higher temperature the mixtures remained in the right-angle helicoidal state with an applied electric field until the helical structure was unwound and the liquid crystal molecules aligned with the field. These results then show that the presence of RM82 and I-651 does not hinder the formation of the Ch_{OH} structure and the response of the composition in sample OB1 is comparable to that measured in prior examinations, where the relative content of CB7CB, CB6OCB, and 5CB was similar to that in OB1.[15] Although not shown here, samples containing up to 4.8 wt% of RM82 were examined prior to polymerization. The oblique helicoidal structure could be field-induced in all samples and this is strong, indirect evidence that $K_{33} << K_{22}$ even when small amounts of RM82 are added to the mixtures. This inference can be later tested by the independent measurement of the K_{22} and K_{33} elastic constants.

The slope for the line representing the notch position as a function of inverse electric field is expected to depend on the composition of the material. Results for two different chiral dopant concentrations have been reported in Ref. 15. There it was shown that, for a given electric field strength, the notch is observed at longer wavelengths for a sample containing a lower amount of S811. The values of the critical fields should also depend on the composition of the mixtures. The critical fields and the pitch, and thus the notch position, are also expected to depend on temperature through the elastic constants.[11] A detailed in investigation of these dependences has not yet been reported in the literature. For each of the compositions used in this investigation, it was possible to select the magnitude of the electric field strength to yield a

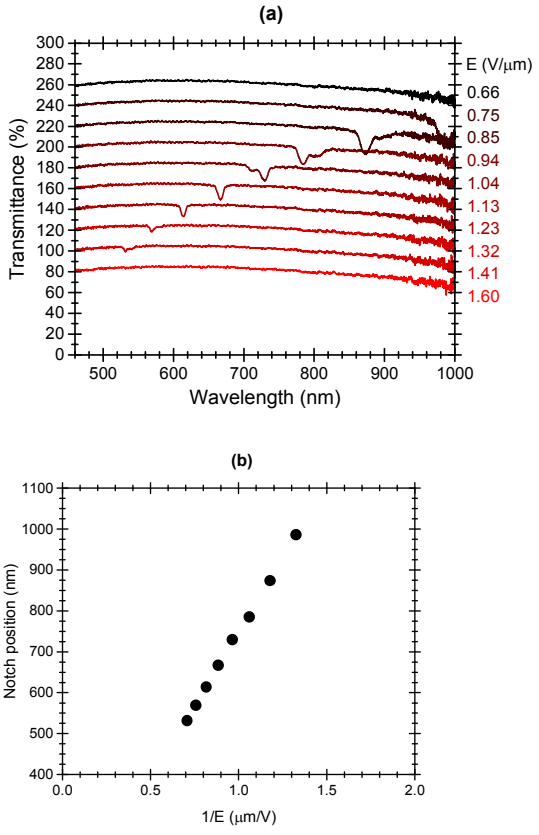

Fig. 3 (a) Transmission spectra of OB1 at 23.0 °C as a function of electric field (square wave at 1.0 kHz). After data collection at a given field strength, the field was set to 3.8 V/μm for a few seconds to bring the sample in the homeotropic state, before it was reduced to the next measurement value. The transmittance scale refers to the first spectrum from the bottom (1.60 V/μm). Each subsequent trace was shifted vertically by 20% on that scale for ease of viewing. (b) Wavelength of the minimum in the transmission spectra in (a) as a function of the inverse of the field amplitude.

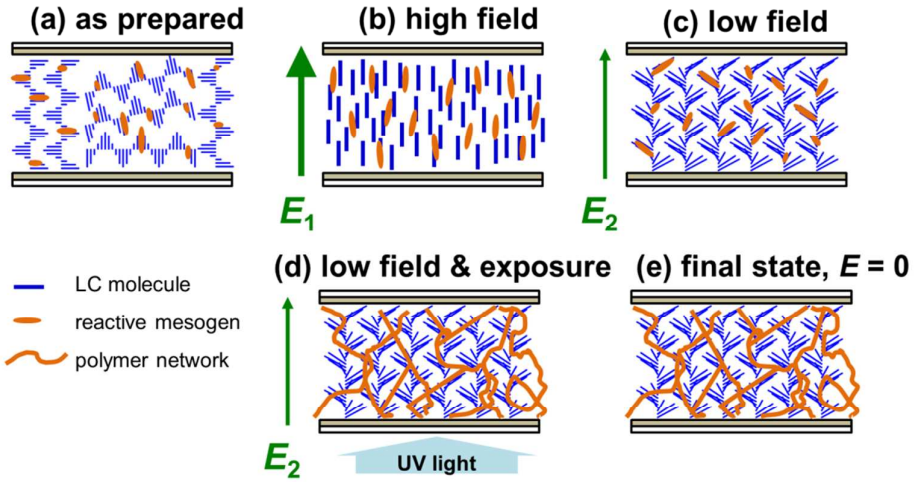

Fig. 4 Scheme for the preparation of polymer stabilized Ch_{OH} systems. (a) The sample is initially in a right-angle N* state, with some disordered or focal conic domains. (b) Homeotropic alignment is induced by an electric field, E_1; both reactive and non-reactive mesogens are reoriented by the field. (c) The oblique helicoidal structure is obtained by decreasing the electric field to E_2, below the upper threshold value. (d) Maintaining the electric field at E_2, the sample is exposed to UV light and a polymer network is formed. (e) If the polymer network is sufficiently strong, the system remains in the oblique helicoidal state after the electric field is switched off.

notch at a desired location in most of the visible range.

A polymer network was then generated by exposing samples while they were in the oblique helicoidal state, following the steps illustrated in Fig. 4. Transmission spectra were recorded before, during, and after the exposure, in order to monitor changes in sample behavior (interval between adjacent acquisitions: 0.5 s). Again, the spectrometer light below 400 nm was blocked, so that only emission from the 365-nm LED contributed to the photopolymerization process. The results for sample OB2/PS-OB2 are shown in Fig. 5. The sample was scattering after preparation and equilibration at the testing temperature (25 °C), as shown in trace (1) of Fig. 5a. Mixtures of LC dimers with chiral dopants usually exhibited many defects and regions with the focal conic texture, with only small Grandjean regions even when the cell surfaces are treated to provide planar alignment (Fig. 4a). These defects and focal conic domains persisted for at least a few hours but it cannot be excluded that longer wait times or annealing cycles may reduce them. The characteristics and energetics of defects in right-angle N* systems containing LC dimers have not yet been studied in detail but they appear to be different from those of N*'s based on calamitic liquid crystals. For example, Salili *et al.* have shown that several modulated structures are possible at zero field when LC dimers are present, and their presence has been attributed to the anomalously small bend elastic constant.[28]

The sample was then brought into the homeotropic state (Fig. 4b) by setting the electric field value to E_1 = 3.8 V/μm (at time t = 0 s in the scale of Fig. 5a) to erase the defects. At time t = 5 s, the voltage amplitude was reduced to E_2 = 1.6 V/μm to induce the formation of the oblique helicoidal structure (Fig. 4c and trace (2) in Fig. 5a). It should be noted that the transition from the homeotropic to the oblique helicoidal state is usually rather slow, as shown by the progressive change in

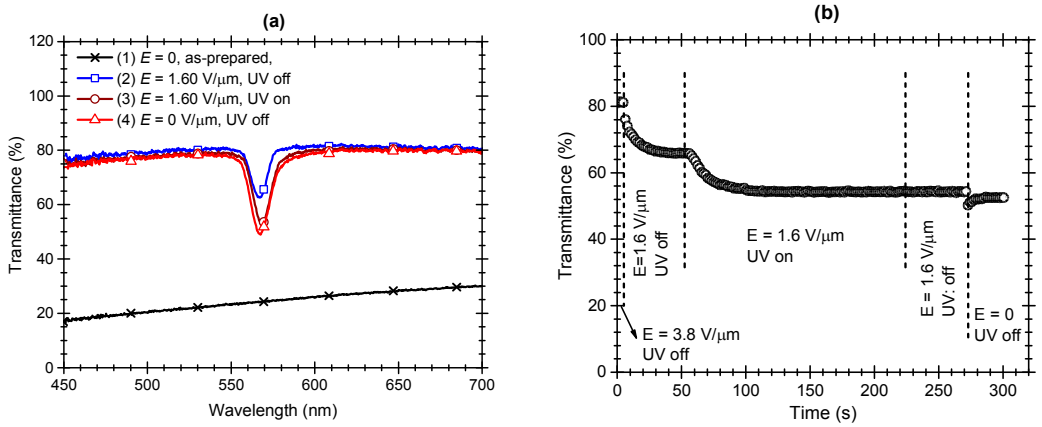

Fig. 5 (a) Transmission spectra of OB2 and PS-OB2 at 25 °C, unpolarized light: (1) OB2, as prepared, no applied field; (2) OB2 with E = 1.60 V/μm; (3) PS-OB2 with E = 1.60 V/μm after 100 s of exposure to UV light (3.5 mW/cm^2); (4) PS-OB2 after exposure (polymerization) and with E = 0 V/μm. (b) Transmittance of the sample at 570 nm as a function of time. The vertical dotted lines separate the various stages of the experiment (all at 25 °C); the electric field amplitude and illumination status are indicated for each.

transmittance at 570 nm in Fig. 5b between 5 s and about 30 s. While the electric field was on, the sample was then exposed to the UV light (3.5 mW/cm^2) (Fig. 4d). During this exposure (from t = 52 to 232 s), the formation of the polymer network transforms OB2 into PS-OB2 (Fig. 5b and trace (3) in Fig. 5a) and the transmittance in the reflective region decreased somewhat. However, little to no change is observable in the transmission of the samples outside this region, suggesting excellent retention of phase during the photopolymerization step. When the field was turned off after polymerization, the reflection was still clearly present (trace (4) in Fig. 5a; the small change in the transmittance value when the field is turned off will be discussed later). Given this evidence, it can be inferred that the LC molecules in the exposed sample PS-OB2 are still arranged in the oblique helicoidal structure (Fig. 4e). An electric field is no longer needed to maintain the molecule in this conformation, because of the presence of the polymer network. This structure is stable for periods of days to weeks when the sample is stored at room temperature. Over time, the samples became scattering because of phase separation of one or more of the low-molecular weight components of the mixture, but the selective reflection band did not disappear completely.

The behavior observed for PS-OB2 during the polymerization was common to most of the samples tested. In some cases, though, a small shift in the position of the band (typically toward shorter wavelengths) was also observed as photopolymerization progressed, possibly associated with a small change in the refractive index or elastic constant of the material while the polymer network was formed. Also, not all of the samples exhibited an increase in selective reflection after polymerization relative to prior to polymerization, as PS-OB2 does (trace (3) relative to (2) in Fig. 5a). The reason for this additional attenuation is not understood at the moment. One possibility is that this may result from a decrease in the number of defects in the sample during the exposure step and related increase in domain sizes. Monitoring of the samples' texture during the exposure step could be used to probe this hypothesis.

The position of the selective reflection, and thus the magnitude of the pitch of the oblique helicoid, is dictated by the amplitude of the electric field in steps (c)-(d) of the preparation procedure. Thus, stabilized samples with different pitches can be obtained from the same starting mixture by selecting the desired field strength during the photopolymerization. Transmission spectra for two such polymer stabilized Ch_{OH} samples are shown in Fig. 6a; photopolymerization was conducted with E = 1.6 V/μm for PS-OB3 and E = 1.3 V/μm for PS-OB4, and with the same exposure conditions as PS-OB2. It can be seen that in both cases the selective reflections, corresponding to bandgap modes, are clearly present when the stabilized samples are probed at zero field. The transmission minimum is observed at 580 nm for PS-OB3 and 687 nm for PS-OB4. Comparison of the spectra for PS-OB3 (Fig. 6a) and PS-OB2 (Fig. 5a, trace (4)) shows reasonably good repeatability of the sample fabrication process, as these were obtained from the same mixture and polymerized under the same conditions.

Images obtained in reflection mode for these two samples are shown in Fig. 6b and 6c. The texture appears rather uniform over large area, with a reflection color consistent with the position of the band observed in the transmission spectra (green for PS-OB3 and red for PS-OB4). It can also be noticed that, in both cases, there appears to be small domains with different colors surrounded by the domain with the predominant color. The distribution and sizes of the differently colored domains are not uniform within the exposed area of a given sample and some variation within samples prepared under the same condition was observed. At the boundary between two adjacent domains, the color change is abrupt, not gradual. This could indicate that there are local pitch changes associated with the sample accommodating a different number of repeat units through its thickness, as is also the case in N*. For example, in the case of sample PS-OB3, the peaks of the reflection bands in adjacent domains with different color were observed at λ' = 562.8 and λ'' = 573.0 nm (as measured with a microspectrometer with a spot size of 20 μm × 20 μm and a resolution of 1.5 nm). If L is the cell thickness (20 μm) and n_{av} the average refractive index (about 1.65[15]), the number of repeat units in the domain with band at λ' is: $h = n_{av} L/\lambda'$ = 59 and the expected wavelength shift between domains with h and h-1 repeat units would be: $\Delta\lambda = n_{av} L /[h (h\text{-}1)]$ = 9.6 nm, close to the experiment value (10.8 nm). A quantitative analysis of results on a larger number of samples and domain colors will be used to test this interpretation against other possible causes for the discrete changes in reflection color (such as inhomogeneities in the substrates) and the findings will be reported separately.

The bands associated with selective reflection of the stabilized Ch_{OH} samples are usually relatively narrow (15-20 nm full width at half maximum), as can be seen in Fig. 6a, and similar bandwidths were observed on the samples before forming the polymer network. Notably, the bandwidths of the selective reflection modes recorded during this investigation were often significantly narrower than those in the original reports on Ch_{OH}.[14, 15] For example, widths were found to be between 25 and 65 nm for bands in the 500-900 nm range in Ref. 15. Due to the small effective birefringence associated with the oblique helicoidal structure as a result of the molecular tilt toward the helical axis, the bandwidth of the selective reflection mode is expected to be narrower than in N* systems with a similar composition and band position. The smaller bandwidths observed in the samples discussed here may indicate that larger domains and fewer defects were present than in the previous investigation,[15] either because of the smaller cell thickness (20 instead of 50 μm) or of the type of surface alignment (planar instead of homeotropic).

After polymerization, the reflective state at zero field was retained down to at least 19 °C (the lowest temperature tested), suggesting a depression of the temperature for the transition from the liquid crystal to the solid state. The samples appeared to become isotropic in the same temperature range as the mixtures prior to polymerization.

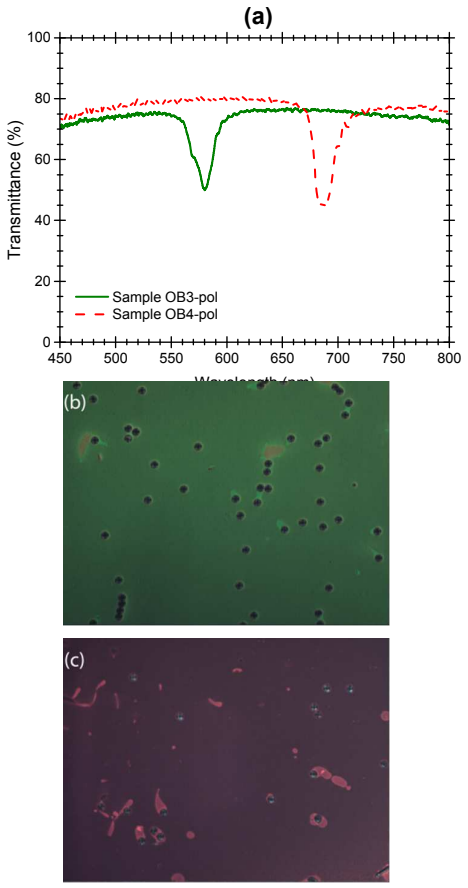

Fig. 6 (a) Transmission spectra of PS-OB3 and PS-OB4 at 25 °C and no applied field, using unpolarized light. (b-c) Reflection mode micrographs recorded at room temperature with polarizer and analyzer oriented along the horizontal and vertical directions for (b) sample PS-OB3 and (c) sample PS-OB4. Image dimensions: 1090 μm × 820 μm. The dark circles are spacer beads (20 μm).

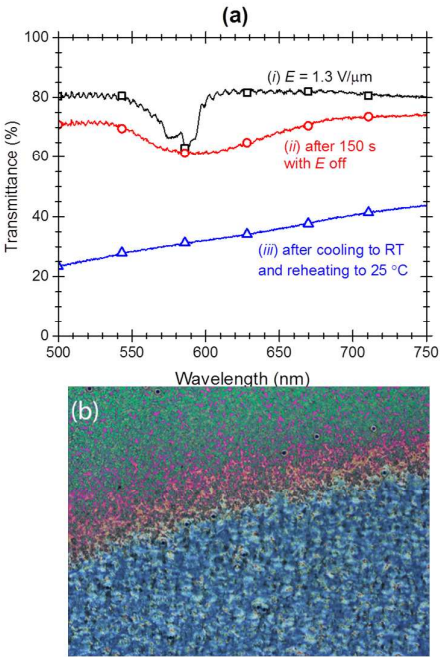

Fig. 7 (a) Transmission spectra (unpolarized light) of PS-OB5 at 25 °C: (*i*) spectrum at the end of the exposure, before the field was turned off; (*ii*) spectrum 150 s after switching off the voltage; (*iii*) spectrum at zero field after cooling the sample to room temperature and reheating it to 25 °C. (b) Transmission mode micrograph of PS-OB5, recorded at room temperature with polarizer and analyzer oriented along the horizontal and vertical directions. The curved transition region in the image separates the area that was exposed to UV light (bottom) from the one that was not exposed (top). The image brightness was increased by software after the data collection. Image dimensions: 1160 μm × 870 μm.

However, the samples typically became scattering at temperatures above 35-40 °C and the transmission notch became less deep, an indication that the polymer network was deformed at these temperatures. This deformation was not fully reversible, as samples remained partly scattering after cooling back to room temperature. The behavior of polymer stabilized Ch_{OH}'s as a function of temperature will have to be further analyzed to determine the operating range of the devices.

The ability to retain the Ch_{OH} state absent an electric field was found to be dependent on the concentration of the polymer network. Polymer stabilized samples with spectral characteristics and textures of the type described above were observed for starting mixtures containing 2.8% to 4.8% of RM82 monomer, with R811, S811, or TADDOL as chiral dopants. However, the polymer network did not provide sufficient structural integrity to stabilize the oblique helicoidal structure in the absence of an electric field when 2.2% RM82 was used (sample PS-OB5). Before exposure to UV light, the OB5 sample assumed the Ch_{OH} structure with selective reflection at 588 nm for E = 1.32 V/μm. The sample was then exposed to UV light at 4.3 mW/cm^2 for 180 s, during which time the bandgap mode remained visible but experienced some changes in shape and depth relative to the pristine sample (see Fig. 7a, trace (*i*) for the spectrum observed at the end of the exposure). When the electric field was turned off at the end of the exposure, the band broadened within a few seconds and the sample became scattering over time (Fig. 7a, trace (*ii*)). Ultimately, the selective reflection disappeared altogether (trace (*iii*)). When viewed under a polarizing microscope, a disordered texture was apparent and variations in color or brightness could be identified between domains extending over only tens of microns (Fig. 7b, bottom part). This texture is clearly different from the one displayed in Fig. 6b-c. Evidence that polymerization took place can be garnered from the texture of the sample in areas that were not exposed to UV light (top part of image Fig. 7b), where the sample was, for the most part, disordered, but small planar domains, which formed when the electric field was switched off, were also present. The PS-OB5 sample also underwent a phase transition as it equilibrated to room temperature from 25 °C, whereas samples fabricated from mixtures containing larger amounts of RM82 did not exhibit phase transitions between 19 and 25 °C after the polymerization step.

The structural robustness of the polymer network was also varied by decreasing the exposure dose at a fixed content of RM82, which should lead to incomplete polymerization and lower cross-linking densities. The effects of exposure dose are illustrated in Fig. 8, where results for PS-OB3 (high dose) and PS-OB6 (low dose) are compared. The two samples differed in at least two respects: the recovery to the new "equilibrium state" at zero field of the polymerized sample after a field of 1-4 V/μm amplitude was applied for at least a few seconds, and the microscopic texture. As seen in Fig. 8a, transmission spectra for PS-OB3 after the electric field had been cycled on and off a few times were almost identical. Instead, the shape and depth of the transmission notch changed every time the field was turned off for PS-OB6, for which polymerization was carried out at about 20% of the dose used for PS-OB3. We will show in Section 3.2 that polymerized samples respond to electric fields. The results in Fig. 8a-b show that the recovery of the electro-optical response is complete only if the polymer network is sufficiently strong. The low-dose sample PS-OB6 exhibited mainly the texture characteristic of the oblique helicoidal state (compare Fig. 8c with Fig. 6b); however, regions with a whitish tinge and diffuse boundaries are also visible in some areas (as in the top-right corner of Fig. 8c). These regions may indicate that there is some disorder in the direction of the oblique helicoidal axis or in the tilt angle, laterally or through the sample thickness.

3.2 Electro-optical properties of polymer stabilized samples

The electro-optical response of samples in which polymer stabilization enabled the retention of the oblique helicoidal structure at zero field was examined. The results for two samples, PS-OB2 and PS-OB7 (the latter containing TADDOL as chiral dopant) are shown in Fig. 9. It can be seen that the depth of the notch in transmission decreases with increasing electric field amplitude in both samples. No significant change in the position of the band was identified. This is clearly different from the behavior of the oblique helicoidal state in low-molecular weight systems,[15] where the band position shifts to shorter wavelengths with increasing electric field strength as discussed in Section 1 (see also Fig. 3). It is not unusual that polymer stabilized samples exhibit different electro-optic responses relative to those of materials without embedded polymer, and new effects and potential applications have been enabled by exploiting polymer stabilization.[20, 29] In the present case it is remarkable that a polymer content of only 3-4% is (i) sufficient to introduce a new equilibrium state in the system and (ii) completely disable the electro-optic response of the small-molecule analogue. Ongoing research will continue to explore and optimize the composition of the polymer network in an effort to realize tunability of the selective reflection in these materials.

The spectral changes in response to electric fields are fully reversible if the polymer network is strong enough, as discussed above (Fig. 8a). A small decrease in the off-band transmittance on the low-wavelength size of the bandgap mode was observed at probing fields of high strength (> 3 V/μm) in some of the samples, possibly because of non-uniform deformations of the polymer network. This change was also reversible and the sample regained the off-band transmittance when the field was turned off. An increase of the polymer content above 5% could help in mitigating this problem (possibly at the expense of an increase in critical field). It was mentioned earlier that a change of the in-band transmittance was observed when the electric field was first turned off after completion of the photopolymerization (traces (3) and (4) in Fig. 5a). That change is consistent with the electro-optic behavior of Fig. 9, where the largest beam attenuation is always seen at zero field in polymer stabilized Ch_{OH} systems.

The decrease in the efficiency of the selective reflection mode with field strength is the manifestation of some form of molecular reorientation that takes place in the polymer stabilized samples when an electric field is applied. The decrease in attenuation could indicate that the tilt angle θ_E in the oblique helicoid decreases with increasing field, which would result in a decrease of the effective birefringence of the material probed at normal incidence. A decrease in tilt angle with increasing electric field is also characteristic of the oblique helicoidal state in the absence of polymer.[11, 14] However, the results in Fig. 9 indicate that there is no

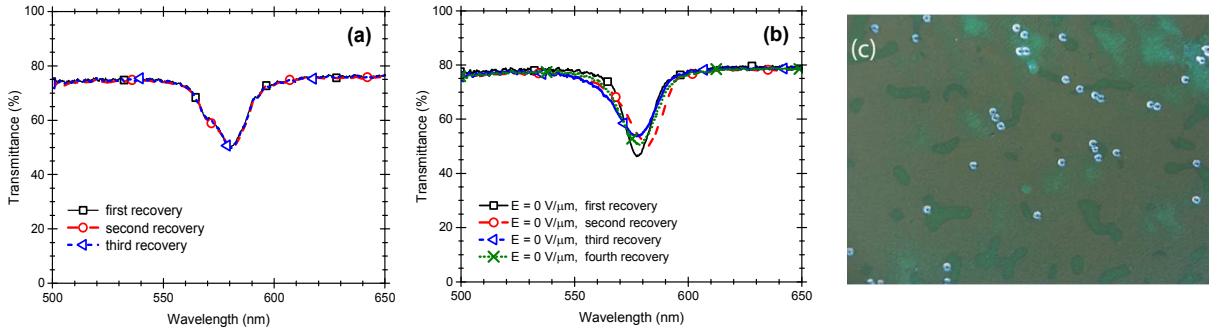

Fig. 8 (a-b) Transmission spectra (unpolarized light) of (a) PS-OB3 and (b) PS-OB6 with no applied field at 25 °C. Between each data collection, a field of E = 3.8 V/μm was applied to the samples for a few seconds and then switched off. (c) Transmission mode micrographs of PS-OB6, recorded at room temperature with polarizer and analyzer oriented along the horizontal and vertical directions. The image brightness was increased by software after recording. The round objects are spacer beads. Image dimensions: 1160 μm × 870 μm.

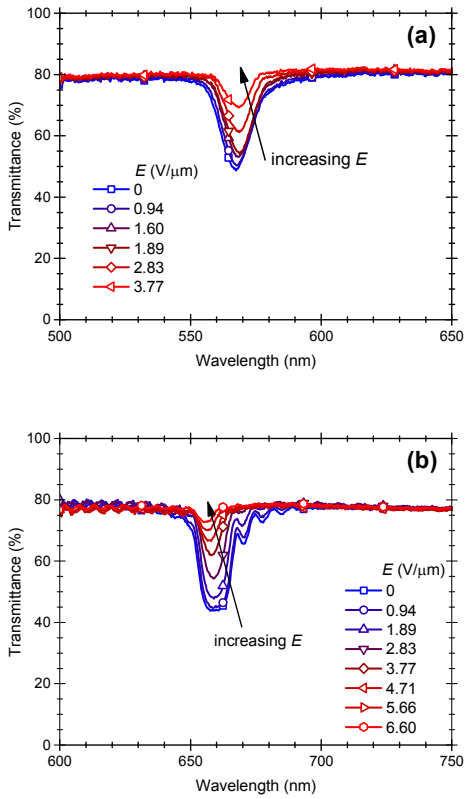

Fig. 9 Transmission spectra of polymer stabilized samples as a function of electric field: (a) PS-OB2; (b) PS-OB7. Data collected with unpolarized light and at 25 °C.

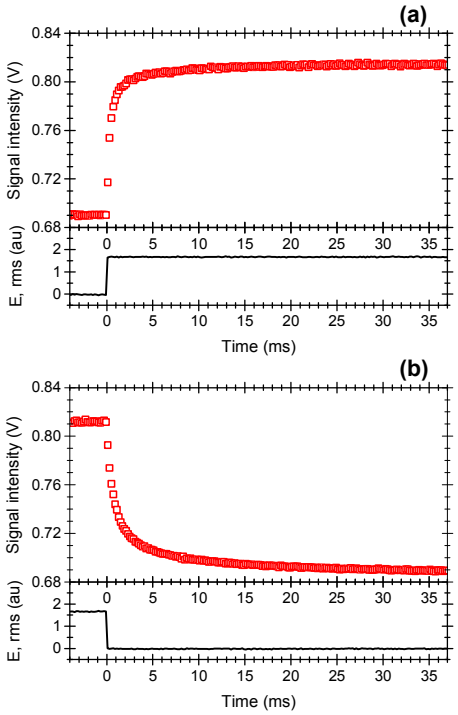

Fig. 10 Intensity of light transmitted by a polymer stabilized sample, PS-OB8, as a function of time when an electric field (3.6 V/μm, square wave at 4 kHz) is turned on (a) and off (b). Data collected at 0.2 ms intervals with unpolarized light and at room temperature. The top panel in each graph is the intensity of the transmitted light (at 710 nm, 10 nm bandwidth); the bottom panel is the relative amplitude value of the applied field.

associated change in the pitch of the helical structure in the presence of a polymer network.

The molecular reorientation and accompanying spectral changes start at electric field amplitudes on the same order as those used initially to generate the oblique helicoidal structure. For example, for OB7, the polymerization step was carried out at E = 1.46 V/μm, yielding a notch at 658 nm, but the oblique helicoidal structure existed up to at least 1.9 V/μm (at higher field, either the selective mode was too weak to be detected or the sample was in the electric-field induced homeotropic state). Significant changes in the notch depth of PS-OB7 were seen going from 0 to 1.9 V/μm (from 44% to 48% transmittance) and the notch almost completely disappeared at three times that amplitude. Thus, the threshold voltage for this class of PSLC devices is not much larger than in small-molecule systems with similar composition.

The variation in transmittance in response to an electric field and the sample recovery after the field is switched off were monitored over time, in order to estimate the response times of the polymer stabilized Ch_{OH} devices. For this experiment, narrow-band filters were used to select the portion of the lamp spectrum centered at the bandgap mode of a given sample. The sample transmittance was detected by a photodiode and recorded on a digital oscilloscope. The results in Fig. 10 are for sample PS-OB8, with a notch centered at 708 nm. It can be seen that the rise and decay times are rather fast. Specifically, for this sample at E = 3.6 V/μm, 90% of the signal change was observed within 2.5 ms after the field was applied and 6.7 ms when the field was switched off. The shape of the rise and decay traces in Fig. 10 follows to a good approximation the sum of two exponential terms, with characteristic times 0.36 and 4.6 ms on the rise side (Fig. 10a) and 0.80 and 6.3 ms on the decay side (Fig. 10b). The rise response times were found to decrease slightly with increasing amplitude of the field, whereas the decay times increased slightly. The response times of the polymer stabilized Ch_{OH} devices are on the order of those observed in other PSLCs devices,[20] and faster than the typical electro-optical response of small-molecule LCs.[30] Results on a wider range of conditions and samples are needed to provide a more quantitative description of the trends as a function of field and for comparisons with other PSLCs.

We also investigated the polarization characteristics of the transmission and reflection spectra of polymer stabilized Ch_{OH} systems. Pairs of samples were prepared starting from mixtures with similar composition but with chiral dopants of opposite handedness (R811 or S811). Photopolymerization was then conducted in each member of the pair using similar field amplitudes and exposure conditions, so as to yield bandgap modes in approximately the same spectral region.

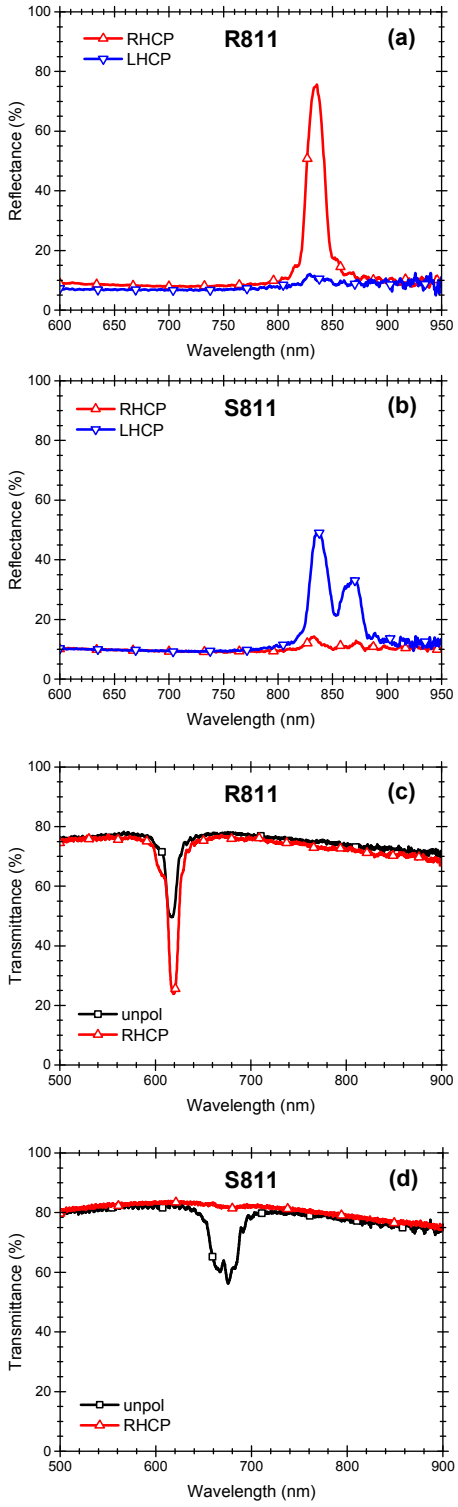

Fig. 11 Spectra of polymer stabilized samples with chiral dopants of opposite handedness for various polarization conditions of the probing light: Reflection spectra of PS-OB1 (a) and PS-OB9 (b) decomposed into the components with RHCP and LHCP (reflectance values relative to that of an aluminum mirror). Transmission spectra of PS-OB10 (c) and PS-OB11 (d) collected with unpolarized light and RHCP light. The chiral dopant (R811 or S811) for each sample is indicated in the corresponding graph.

The reflection spectra of one such pair, PS-OB1 and PS-OB9, are displayed in Fig. 11a-b. These spectra were obtained using unpolarized light incident on the samples and then separating the components with right-handed and left-handed circular polarization (RHCP and LHCP, respectively) in the reflected signal. It can be seen that PS-OB1, which contains R811, exhibits a strong reflection band centered at 835 nm that has RHCP, whereas there is almost no reflection with LHCP. Conversely, sample PS-OB9, containing S811, exhibits reflection with LHCP but not with RHCP. The reflection band of PS-OB9 has a double-peak structure (837 and 868 nm), as a result of the coexistence of domains with different pitches in the probed area. A mixture of domains or the presence of defects is also responsible for the lower peak reflectance in the case of PS-OB9 relative to PS-OB1.

The transmission spectra of another pair of samples with different handedness are shown in Fig. 11c-d. When the samples are probed with unpolarized light, a notch band is clearly visible in both PS-OB10 and PS-OB11 (centered at 617 and 670 nm, respectively). However, PS-OB11, which contains S811, is transparent to light with RHCP. The R811-containing PS-OB10, instead, exhibits very strong attenuation of light with RHCP. These results show that, at normal incidence, the oblique helicoidal structure effectively reflects only light with one sense of circular polarization, while the other polarization is fully transmitted. This polarization selectivity is the same as for N* systems and for LC systems in the smectic C phase. The minimum transmittance in the attenuation band was about 20% for RHCP in Fig. 11c and thus even this polarization state does not appear to be completely blocked, as instead should be expected in the ideal case of a chiral structure. The incomplete blocking of RHCP light in this case could results from the small effective birefringence of Ch_{OH} structures, which is also linked to narrow width of the band, and the presence of domain boundaries and other defects in the samples.

Conclusions

The properties of the oblique helicoid, Ch_{OH}, structure of liquid crystals have only recently been described experimentally by Lavrentovich and coworkers[11, 14, 15] after the realization that in some LC dimers the elastic constants satisfy the requirement identified 50 years ago for the existence of the structure ($K_{33} < K_{22}$).[13] In the Ch_{OH} state, the pitch and the tilt angle of the director relative to the helical axis depend on the magnitude of the electric field (directed along the helical axis). In the absence of the electric field, the systems assume the traditional right-angle helicoidal configuration. We have now shown that, when 3-5 wt% of a reactive mesogen is present in the LC mixture and its polymerization is carried out while the system is in the Ch_{OH} state, this state is stabilized by the polymer network and becomes the new equilibrium configuration of the LC, being observable after the electric field is turned off. The strength of the electric field during the polymerization step determined the pitch of the Ch_{OH}. Once the polymer network is formed, the pitch was locked and

could no longer be controlled by the field. In the polymer stabilized Ch_{OH} structures described here, the field strength only affected the magnitude of the selective reflectance, with response times on the order of ms.

This method allows the fabrication of devices with the same overall polarization characteristic as systems based on the N* state, but with narrower bands, due to the small effective birefringence for light propagating along the axis of the oblique helicoid. When polymer stabilized, this state is stable at zero field, but the reflection efficiency can be controlled over a grey scale by the field. This combination of properties could set polymer stabilized Ch_{OH} systems apart from other LC-based devices and may find end use applications in new types of devices. To realize implementation in devices, further improvements in the fabrication process of polymer stabilized Ch_{OH} devices are necessary. For example, with the materials and process employed here, the devices are still often nonuniform in both texture and optical properties over large areas.

Conflicts of interest

There are no conflicts to declare.

Acknowledgements

This work was supported by the Air Force Office of Scientific Research and the Materials and Manufacturing Directorate of the Air Force Research Laboratory.

Notes and references

1. G. R. Luckhurst, *Macromol. Symp.*, 1995, **96**, 1.
2. P. J. Barnes, A. G. Douglass, S. K. Heeks and G. R. Luckhurst, *Liq. Cryst.*, 1993, **13**, 603.
3. P. A. Henderson and C. T. Imrie, *Liq. Cryst.*, 2011, **38**, 1407.
4. V. Borshch, Y. K. Kim, J. Xiang, M. Gao, A. Jákli, V. P. Panov, J. K. Vij, C. T. Imrie, M. G. Tamba, G. H. Mehl and O. D. Lavrentovich, *Nat. Commun.*, 2013, **4**, 2635.
5. K. Adlem, M. Čopič, G. R. Luckhurst, A. Mertelj, O. Parri, R. M. Richardson, B. D. Snow, B. A. Timimi, R. P. Tuffin and D. Wilkes, *Phys. Rev. E*, 2013, **88**, 022503.
6. C. Meyer, G. R. Luckhurst and I. Dozov, *J. Mater. Chem. C*, 2015, **3**, 318.
7. D. A. Paterson, J. P. Abberley, W. T. A. Harrison, J. M. D. Storey and C. T. Imrie, *Liq. Cryst.*, 2017, **44**, 127.
8. G. Cukrov, Y. M. Golestani, J. Xiang, Y. A. Nastishin, Z. Ahmed, C. Welch, G. H. Mehl and O. D. Lavrentovich, *Liq. Cryst.*, 2017, **44**, 219.
9. M. J. Bradshaw, E. P. Raynes, J. D. Bunning and T. E. Faber, *J. Phys. (Paris)*, 1985, **46**, 1513.
10. M. Hara, J.-I. Hirakata, T. Toyooka, H. Takezoe and A. Fukuda, *Mol. Cryst. Liq. Cryst.*, 1985, **122**, 161.
11. J. Xiang, S. V. Shiyanovskii, C. Imrie and O. D. Lavrentovich, *Phys. Rev. Lett.*, 2014, **112**, 217801.
12. G. Babakhanova, Z. Parsouzi, S. Paladugu, H. Wang, Y. A. Nastishin, S. V. Shiyanovskii, S. Sprunt and O. D. Lavrentovich, *Phys. Rev. E*, 2017, **96**, 062704.
13. R. B. Meyer, *Appl. Phys. Lett.*, 1968, **12**, 281.
14. J. Xiang, S. V. Shiyanovskii, Y. Li, C. T. Imrie, Q. Li and O. D. Lavrentovich, *Proc. SPIE*, 2014, **9182**, 91820P.
15. J. Xiang, L. Yannian, Q. Li, D. A. Paterson, J. M. D. Storey, C. T. Imrie and O. D. Lavrentovich, *Adv. Mater.*, 2015, **27**, 3014.
16. S. M. Salili, J. Xiang, H. Wang, Q. Li, D. A. Paterson, J. M. D. Storey, C. T. Imrie, O. D. Lavrentovich, S. N. Sprunt, J. T. Gleeson and A. Jákli, *Phys. Rev. E*, 2016, **94**, 042705.
17. J. Xiang, A. Varanytsia, F. Minkowski, D. A. Paterson, J. M. D. Storey, C. T. Imrie, O. D. Lavrentovich and P. Palffy-Muhoray, *Proc. Natl. Acad. Sci. U. S. A.*, 2016, **113**, 12925.
18. R. A. M. Hikmet and J. Lub, *Prog. Polym. Sci.*, 1996, **21**, 1165.
19. R. A. M. Hikmet, *Liq. Cryst.*, 2006, **33**, 1410.
20. I. Dierking, *Adv. Mater.*, 2000, **12**, 167.
21. D.-K. Yang and S.-T. Wu, *Fundamentals of Liquid Crystal Devices*, 2nd edn., John Wiley & Sons, 2015.
22. Y. K. Fung, A. Borštnik, S. Zumer, D.-K. Yang and J. W. Doane, *Phys. Rev. E*, 1997, **55**, 1637.
23. R. A. M. Hikmet, *J. Appl. Phys.*, 1990, **68**, 4406.
24. R. A. M. Hikmet and R. Howard, *Phys. Rev. E*, 1993, **48**, 2752.
25. R. E. Kraig, P. L. Taylor, R. Ma and D.-K. Yang, *Phys. Rev. E*, 1998, **58**, 4594.
26. J. Guo, H. Cao, J. Wei, D. Zhang, F. Liu, G. Pan, D. Zhao, W. He and H. Yang, *Appl. Phys. Lett.*, 2008, **93**, 201901.
27. M. E. McConney, V. P. Tondiglia, J. M. Hurtubise, L. V. Natarajan, T. J. White and T. J. Bunning, *Adv. Mater.*, 2011, **23**, 1453.
28. S. M. Salili, R. R. Ribeiro de Almeida, P. K. Challa, S. N. Sprunt, J. T. Gleeson and A. Jákli, *Liq. Cryst.*, 2017, **44**, 160.
29. D. K. Yang, in *Liquid Crystals Beyond Displays*, ed. Q. Li, 2012, pp. 505-523.
30. P. Yeh and C. Gu, *Optics of Liquid Crystal Displays*, Wiley, New York, 1999.

Polymer stabilization of cholesteric liquid crystals in the oblique helicoidal state

Mariacristina Rumi, Timothy J. Bunning and Timothy J. White

TOC text:

After polymer stabilization, the oblique helicoidal cholesteric state in mixtures containing CB7CB is stable without any applied electric field.

TOC graphic: